University of HUDDERSFIELD

University of Huddersfield Repository

Wang, Xue, Xu, Qiang, Yu, Shu-min, Hu, Lei, Liu, Hong and Ren, Yao-yao

Laves-phase evolution during aging in 9Cr-1.8W-0.5Mo-VNb steel for USC power plants

Original Citation

Wang, Xue, Xu, Qiang, Yu, Shu-min, Hu, Lei, Liu, Hong and Ren, Yao-yao (2015) Laves-phase evolution during aging in 9Cr-1.8W-0.5Mo-VNb steel for USC power plants. Materials Chemistry and Physics, 163. pp. 219-228. ISSN 0254-0584

This version is available at http://eprints.hud.ac.uk/id/eprint/25730/

The University Repository is a digital collection of the research output of the University, available on Open Access. Copyright and Moral Rights for the items on this site are retained by the individual author and/or other copyright owners. Users may access full items free of charge; copies of full text items generally can be reproduced, displayed or performed and given to third parties in any format or medium for personal research or study, educational or not-for-profit purposes without prior permission or charge, provided:

- The authors, title and full bibliographic details is credited in any copy;
- A hyperlink and/or URL is included for the original metadata page; and
- The content is not changed in any way.

For more information, including our policy and submission procedure, please contact the Repository Team at: E.mailbox@hud.ac.uk.

http://eprints.hud.ac.uk/

Laves-phase evolution during aging in 9Cr-1.8W-0.5Mo-VNb steel for USC power plants

Xue Wang [a)*], Qiang Xu [b)], Shu-min Yu [a)], Lei Hu [a)], Hong Liu [c)], Yao-yao Ren [a)]

[a]*School of Power and Mechanics, Wuhan University, Wuhan 430072, China*

[b]*School of Computing and Engineering, The University of Huddersfield, Huddersfield, HD1 3DH, England*

[c]*DongFang Boiler Group Co.,Ltd.，Zigong 643001, China*

Accepted version, and the revised version was published in Materials Chemistry and Physics, 163. pp. 219-228.

ISSN 0254-0584

Abstract − Laves-phase precipitation and coarsening of tungsten strengthened 9% Cr steel under thermal aging at 923K up to 8000 h was reported in this paper, where the information of the evolution of mean particle size, the number density, the volume fraction of Laves-phase precipitates and the partition coefficients of W and Mo in the matrix over the aging time were determined. The change of hardness over time was also measured. The main results of this investigation were: 1) Laves-phase nucleates and grows rapidly on grain boundaries and lath boundaries within the first 1,500 h of aging time; 2) the coarsening of Laves-phase is much faster than that of $M_{23}C_6$ carbides, meanwhile it demonstrates the two stages characteristics and kinetics of Laves-phase nucleation and growth which were determined experimentally; 3)The precipitation of Laves-phase produces a pronounced matrix depletion of W and Mo atoms; and 4) The precipitated Laves-phase gives rise to weaker precipitation strengthening in comparison with $M_{23}C_6$ carbides, and causes the loss of hardenss and creep strength due to the

Corresponding author. Tel.: +86 13554693820; fax: +86 02768772253.

E-mail address: wxue2011@whu.edu.cn (Xue Wang)

depletion of Mo and W from the solid solution. This paper contributes to the knowledge of kinetics of Laves-phase precipitation and coarsening, as well as understanding the creep damage broadly.

Keywords: Alloys; Anealing; Precipitation; Electron microscopy; Microstructure

Corresponding author. Tel.: +86 13554693820; fax: +86 02768772253.

E-mail address: wxue2011@whu.edu.cn (Xue Wang)

1. Introduction

Recently, Demands on the reduction of CO_2 gas emission have been the driving force in development of ultra supercritical (USC) power plants in China and Europe[1-2]. The high-strength 9Cr ferritic heat-resistant steels containing W as a substitute for a part of Mo, such as 9Cr-0.5Mo-1.8WVNb steel (ASME C.C.2179 P92), are key materials for thick section components at temperatures up to 625 ℃ in USC boilers [3]. Recently, 10^5 h creep rupture strength for the P92 steel had been questioned mainly in view of the microstructural instability during long term service at high temperatures above 600 ℃, and as a result its allowable tensile stress was revised in Europe, U.S. and Japan in 2007, 2006 and 2005, respectively [4].

The Laves-phase plays a complicated and controversial role affecting and/or determining the creep strength of high Cr steels. Firstly, the precipitation of Laves-phase leads to a depletion of Mo and W in the matrix, and thereby reduces the solid solution hardening effect in 9-12% Cr steels [5, 6]; the fine Laves-phase particles contribute to precipitation strengthening and decrease the creep rate in the primary and transient creep region, however, the subsequent coarsening of Laves-phase reduces the precipitation strengthening effect [7]. Secondly, Laves-phase precipitates on lath boundaries in TAF650 steel are conducive to the retardation of lath structure's recovery and enhance the creep rupture strength compared with that on grain boundaries and packet boundaries in Mod.9Cr-1Mo steel [8]. Thirdly, the final rupture is controlled by cavity which is strongly associated with Laves-phase. Recently, the authors [9] have briefly summarized the effect of creep cavity, and also note the report of Lee et al [10] on stress rupture of P92 steel as: 1) the steel shows ductile to brittle transition with increasing rupture life, and the breakdown is in accordance with the onset of brittle intergranular fracture; 2) creep cavities are nucleated at coarse precipitates of Laves-phase along grain boundaries. It was further suggested that these findings can explain the breakdown of creep strength. Laves-phase precipitates and grows during creep exposure. Coarsening of Laves-phase particles over a critical size triggers the cavity formation and the consequent

brittle intergranular fracture. The brittle fracture causes the breakdown. The coarsening of Laves-phase can be detected non-destructively by means of hardness testing of the steel exposed to elevated temperature without stress [10]. The authors [11] have also noted the cavitation of P92 weld is associated with the Laves-phase.

Thus, in order to provide a systematic and definite understanding of that process and the creep damage and final rupture, it is necessary to investigate sequentially that 1) the Laves-phase precipitation and coarsening during the thermal exposure; 2) the Laves-phase precipitation and coarsening under creep (both uniaxial and multi-axial states of stress); 3) the cavitation under creep (both under uniaxial and multi-axial states of stress). This paper reported a detailed investigation of Laves-phase precipitation and coarsening over time. The results of the evolution of the mean size, the number density and the volume fraction of Laves-phase precipitates and partition coefficients of W and Mo in the matrix over time were obtained.

2. Experimental procedure

2.1. Investigated materials

The material investigated was taken from a thick section pipe (325mm outer diameter and 40mm wall thickness) originally supplied by V&M corporation. The compositions of the steel are shown in Table 1. The material had been annealed and air cooled, followed by tempering at 1053 K for 6 h. Then the samples were isothermally aged at 923 K for 100 h, 500 h, 1000 h, 1500 h, 2000 h, 2500 h, 3000 h, 5000 h and 8000 h, respectively. The hardness of the aged specimens was measured using a Brinell hardness tester with a force of 187.5 kgf. The microstructures of as-aged material were observed by optical microscopy. Specimens were prepared by mechanical polishing followed by etching in a solution of ethanol(100 ml), hydrochloric acid(5 ml) and picric acid(1g) at room temperature.

Table 1. Chemical compostions of the investigated P92 steel（wt.%）

C	Si	Mn	Cr	Mo	Ni	W	V	Nb	N	B	S	P	Fe
0.12	0.21	0.43	8.84	0.50	0.16	1.67	0.21	0.067	0.042	0.0033	0.004	0.014	Bal.

2.2. SEM-BSE

SEM-BSE was chosen over the Energy filtered transmission electron microscope (EFTEM) due to its capability of detecting and distinguishing the second phases. Energy filtered transmission electron microscope (EFTEM) offers this similar capability and has been proved to be very useful when applied to 9-12% Cr steel [12], however, this method is not suitable for Laves-phase because of its large precipitate size, only a small number of the specimen area can be observed in one TEM image, and yields poor statistics [13].

In SEM analysis, the thermally aged specimens were observed by backscattered electron (BSE) image, in which Laves-phase was clearly distinguished from $M_{23}C_6$ carbides due to the brighter image of Laves-phase arising from the difference in mean atomic weight. The resolution in the SEM is too low to detect fine MX precipitates, therefore, Laves-phase is uniquely distinguished. Thus it is possible to quantify the change in volume fraction and size distribution of Laves-phase during aging from segmented (binarized) BSE images.

The SEM investigation was performed using a QUANTA400F at 20 keV. Each specimen analysis was usually obtained with more than 5 randomly selected fields analyzed. To find out the optimum SEM parameters (contrast, brightness, etc.) to guarantee comparable and exact quantification results, BSE images at different magnifications (25 and 50 kX) were compared with secondary electron (SE) images with regard to the equivalent circle diameter (ECD) and number of particles. ‘Mean diameter’ was given as the arithmetic mean value of the measured ECD. The ECD measurements of the secondary phase on the basis of BSE images have to be corrected for truncation using the following equation[14]:

$$d_{corr} = \frac{4}{\pi}\bar{d}_{obs} \qquad (1)$$

The corrected median value of the ECD is chosen in this study to describe the precipitate size.

2.3. TEM-EDS

The microstructural evolution of the aged material was investigated by conventional TEM techniques. Thin

foils for observations of change in subgrain width and dislocation density were prepared by twin-jet electropolishing using a solution of 10% perchloric acid and 90% methanol below 223 K. Carbon extraction replicas were prepared from aged specimens in order to avoid matrix effects during chemical analysis of the precipitates by energy dispersive X-ray spectroscope (EDS). Their preparation is as follows: the polished specimens were etched using a solution of 3 mL hydrochloric acid and 1 g picric acid in 100 ml of ethanol, then the etched specimens were carbon coated, and the replicas were released with a solution containing 5% HNO_3 and 90% ethanol. More than 10 dispersion particles were measured by TEM-EDS for $M_{23}C_6$ and Laves-phase of typical aged condition specimens, respectively, and the mean value and the standard deviation of constituent elements in the two precipitates were obtained. The experimentally measured value was compared with theoretical value from thermodynamic equilibrium calculation by Thermo-Calc software.

2.4. Potentiostatic electrolysis

To obtain residues, the specimens were dissolved at the anode in a solution of 75 g potassium chloride and 5 g citric acid in 1000 ml water with the pH value of 3～4. The constant current density was chosen to be between 0.02 and 0.03 A/cm^2, where only the iron matrix dissolves. Details about electrolytically extracted residue method have been reported in Ref.[15]. Later, the chemical composition of extracted residues were analyzed by means of inductively coupled plasma (ICP) mass spectrometry and the partition coefficients of alloying elements in the precipitates or matrix are determined.

3. Results

3.1. Microstructural Change

Fig.1 shows the optical micrographs of specimens after tempering and after aging at 923 K for different times. It can be seen that the constituents of martensite, for example lath, packet and block, appear coarser with increasing the aging times. This is related to the recovery of excess dislocations. However, the martensitic lath is

still clear in the specimen even subjected to aging at 923 K for 8000 h, revealing that the martensitic microstructure in P92 steel exhibits relatively high thermal stability at 923 K.

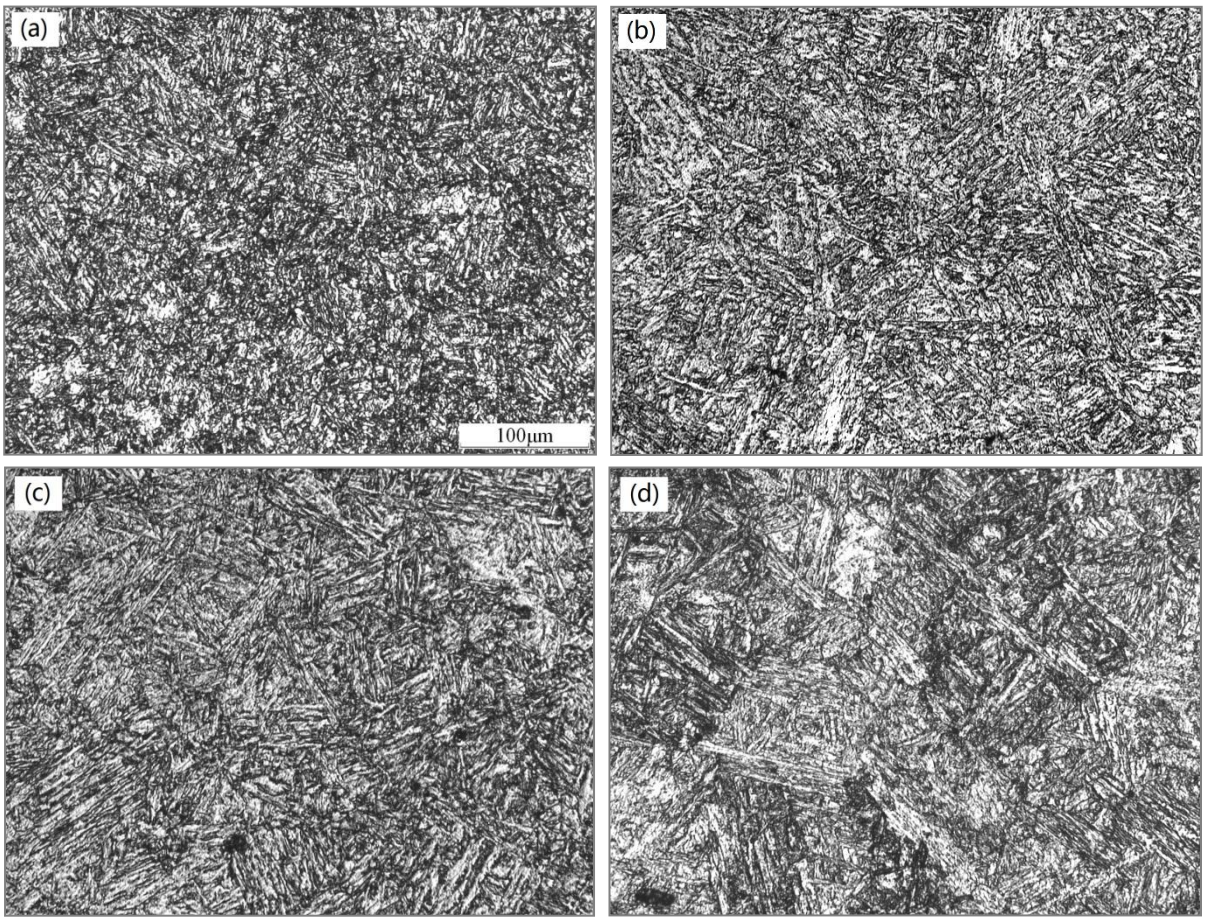

Fig.1 Optical micrographs of P92 steel (a)as received; aged at 923 K for (b)500 h; (c)2000 h; (d)8000 h.

3.2. Quantitative Results of the Laves-phase

For each thermal aging condition more than five SEM-BSE images are produced to visualize precipitates of Laves-phase. For the quantification, the visible and bright precipitates（Laves-phase）in the BSE image are processed to binary images and measured with an image analysis system. The basic principle is shown in Fig.2. The SEM-BSE and the binary images of specimens aged at 923 K for 500 h, 2000 h, 5000 h and 8000 h are on the left and right respectively, as shown in Fig.2. Laves-phase particles are observed on martensite laths boundaries and grain boundaries during aging. The nucleation mechanism for Laves-phase precipitates will be described later. Specimen aged for the first 500 h shows a relative small size and high number density of Laves-phase, while that

aged for 8000 h shows coarse size and fairly lower number density. It should be noted that the size of $M_{23}C_6$ carbides (grey particles) mainly on laths boundaries is much smaller than that of Laves-phase precipitates, and increases slowly during aging up to 8000 h. This indicates that Laves-phase coarsens more rapidly than $M_{23}C_6$ carbides in P92 steel.

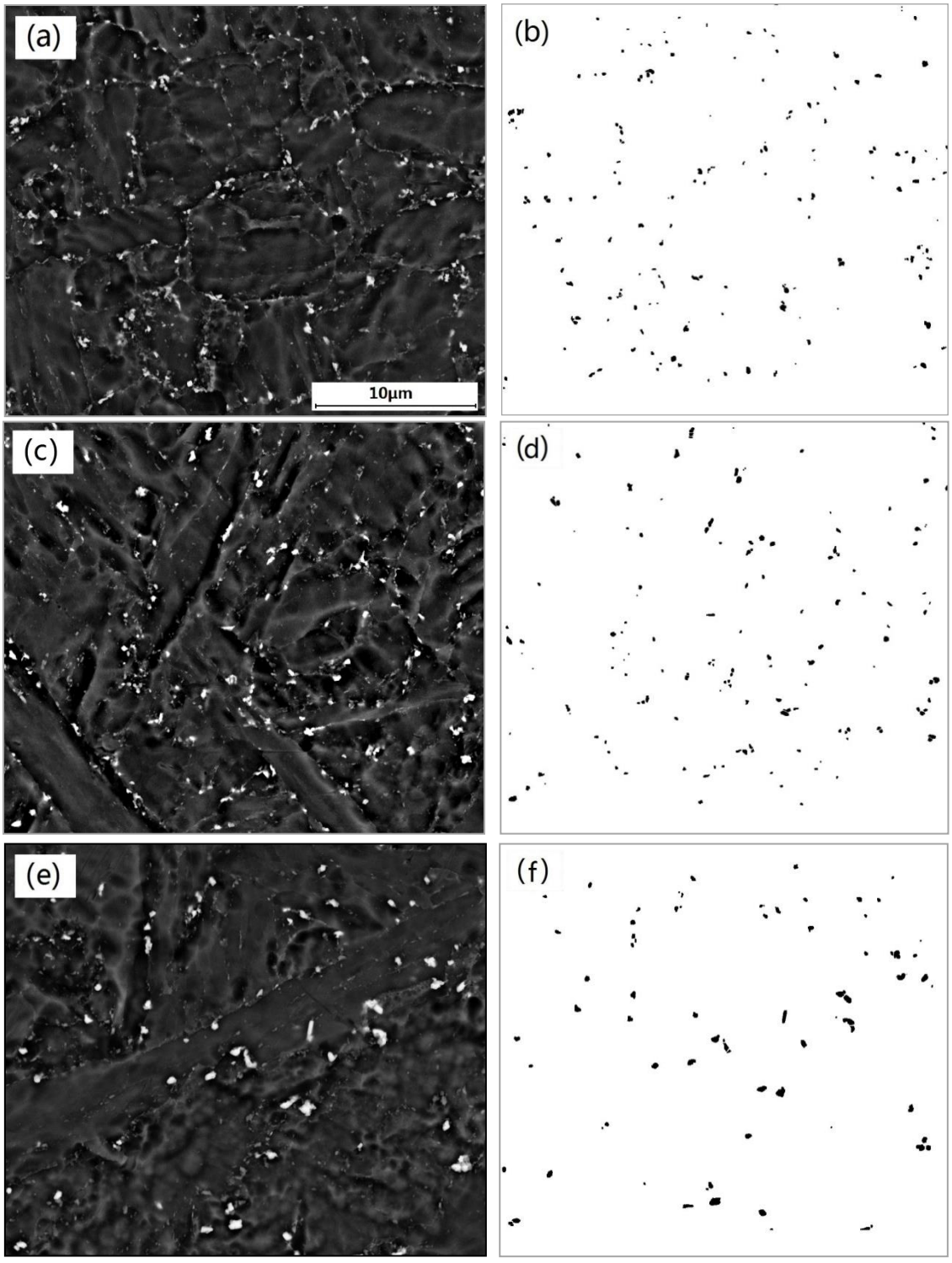

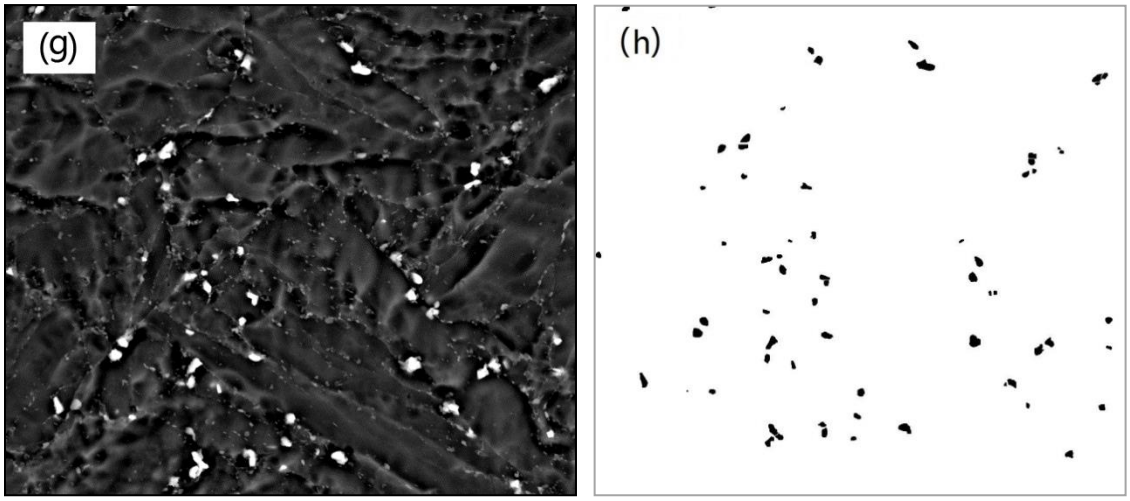

Fig.2 SEM-BSE image and corresponding processed binary image of P92 steels aged at 923 K for 500 h(a) and (b), 2000 h(c) and (d) , 5000 h(e) and (f), 8000 h(g) and (h)

Fig.3（a）-（c）show the area fraction (equal to volume fraction), number density and corrected mean ECD of Laves-phase precipitates as a function of aging time. The area fraction and number density of Laves-phase precipitates increase with increasing time during the first 1500 h of aging. Afterwards, up to 3,000 h, the equivalent diameter seems to be stable while the number density decreases significantly (from $249*10^3$ particles/mm^2 to $189*10^3$ particles/mm^2). Then, coarsening continues up to 8,000 h with the number of particles further dropping to $94*10^3$ particles/mm^2 and the mean ECD increasing from 308 nm to 438 nm. The maximum area fraction of Laves-phase of 0.95% is determined in this investigation, which is very similar to about 1.05 % reported by Dimmler et al [16]. The time for the completion of precipitation is determined as soon as the number density starts to drop and it is found to be 1500 h. This is also similar to that of Ref[16]. However, it is worth to point out that this investigation is based on a high time resolution during exposure and therefore obtains more detailed information of Laves-phase.

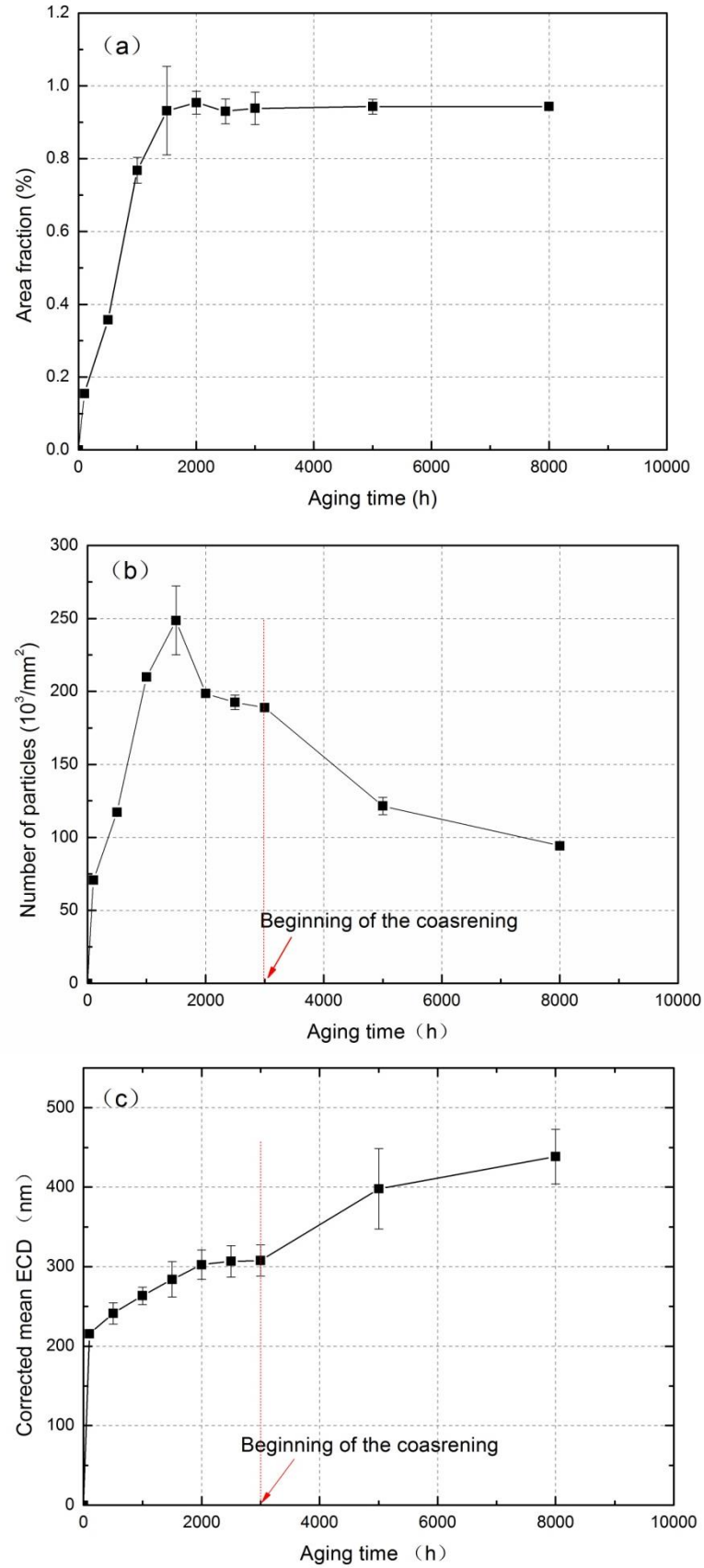

Fig.3 Quantification of Laves-phase precipitates in P92 steel aged at 923 K: （a）area fraction; （b）number of particles and;（c）corrected mean ECD

Fig.4a shows the precipitated phase amounts of equilibrium as a function of temperature calculated by Thermo-Calc in P92 steel with composition given in Table 1. The calculated volume fraction of Laves-phase at 923 K is about 0.58%, which is far lower than the upper limit of 0.95% in this study. The experimental results provided by Dimmler et al[16] and Hättestrand et al[13] also showed that the precipitated volume fraction of Laves-phase in steel P92 aged for 10000 h at 923 K is close to 1.0%. The calculated value is obtained at equilibrium which the Z-phase [Cr（V,Nb）N] forms and fully replaces the MX [（V,Nb）(C,N)] carbonitride, however, no Z-phase is observed during aging at 923 K up to 8000 h. Danielsen[17]have reported observed quantity of Z-phase is still low in P92 steel even after being exposured at 923K for 31000 h. Thus, the Thermo-Calc calculations by suppressing the Z phase altogether are performed to clarify whether the precipitation of Z-phase effects on the amount of Laves-phase, and the results are shown in Fig.4b. It can be seen that the volume fraction of metastable Laves phase is almost the same as that of equilibrium Laves phase at different temperatures, showing that the formation of Z-phase does not affect the amount of Laves-phase in P92 steel. This suggests that the theoretical calculation by Thermo-Calc will overestimate the amount of metastable Laves-phase in P92 steel and other reasons rather than the formation of Z-phase bring about this clear discrepancy.

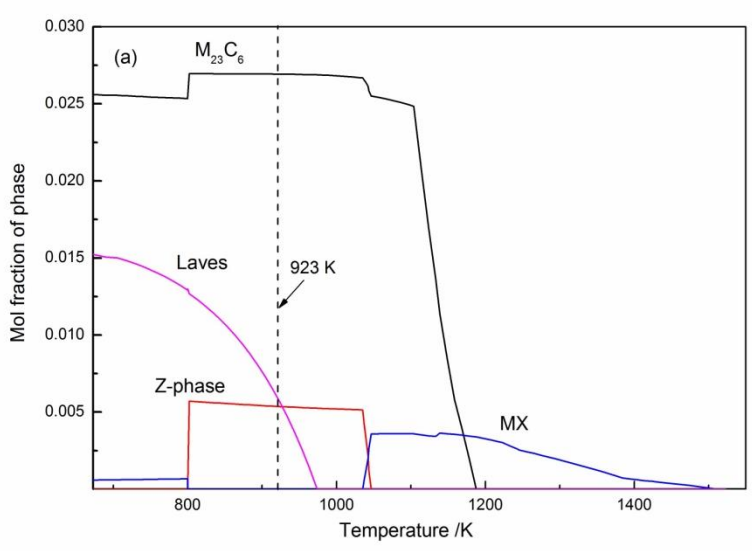

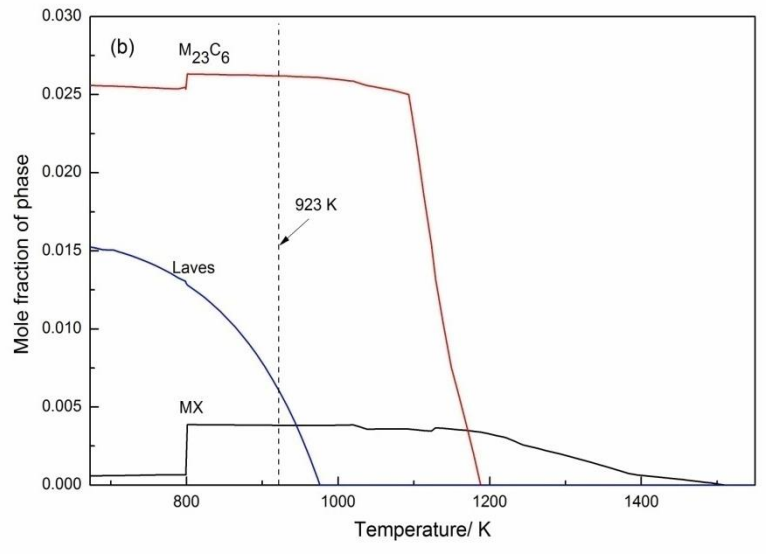

Fig.4 Thermo-Calc calculations showing the phase quantity as a function of temperature in P92 steel: （a）with the precipitation of Z-phase ; （b）without the precipitation of Z-phase

3.3. Results of TEM-EDS

Fig.5 shows the TEM micrographs of the thin foil specimens after tempering and after aging at 923 K for 5000 h. The initial microstructure consists of lath subgrains, which contains a high density of dislocations and fine MX carbonitrides in lath and less fine $M_{23}C_6$ carbides mainly on lath boundaries. Slight decrease in the dislocation density and increase in width of subgrains are observed in the specimen aged for 5000 h compared with the tempered specimen, but the morphology of martensite lath is clear, which further confirms the result observed by OM. In the specimen aged for 5000 h, the MX carbonitrides is still very fine and the coarsening of $M_{23}C_6$ carbides is not obvious, however, some large precipitates can be found, which were analyzed as Laves-phase.

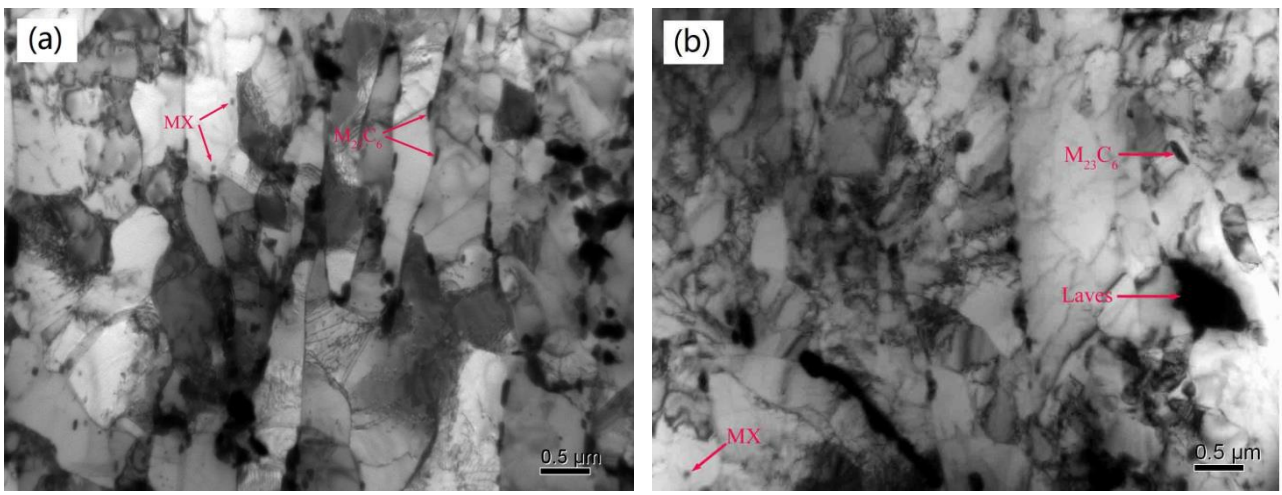

Fig.5 TEM thin micrographs of P92 steel as received (a) and after aged at 923 K for 5000h (b)

Fig.6 shows the TEM micrographs of the carbon extracted replicas of specimens before and after aging for 500 h, 2000 h, and 5000 h. The energy-dispersive X-ray analysis (EDS) shows that minor precipitates are rich in V and Nb and indicate the MX carbonitride, and the less fine precipitates are rich in Cr and the large precipitates are riched in Fe and W, corresponding to $M_{23}C_6$ carbides and Laves-phase particles, respectively. Laves-phase does not occur in the tempered specimen (Fig.6a), because the tempering temperature of 1053 K was above its solution temperature. As shown in Fig.6, Laves-phase precipitates in size increases significantly with increasing aging time, showing quicker coarsening in comparion with $M_{23}C_6$ precipitates. The observations taken by SEM have indicated $M_{23}C_6$ carbides coarse slowly during aging at 923 K, this is further confirmed with TEM observations at high magnification.

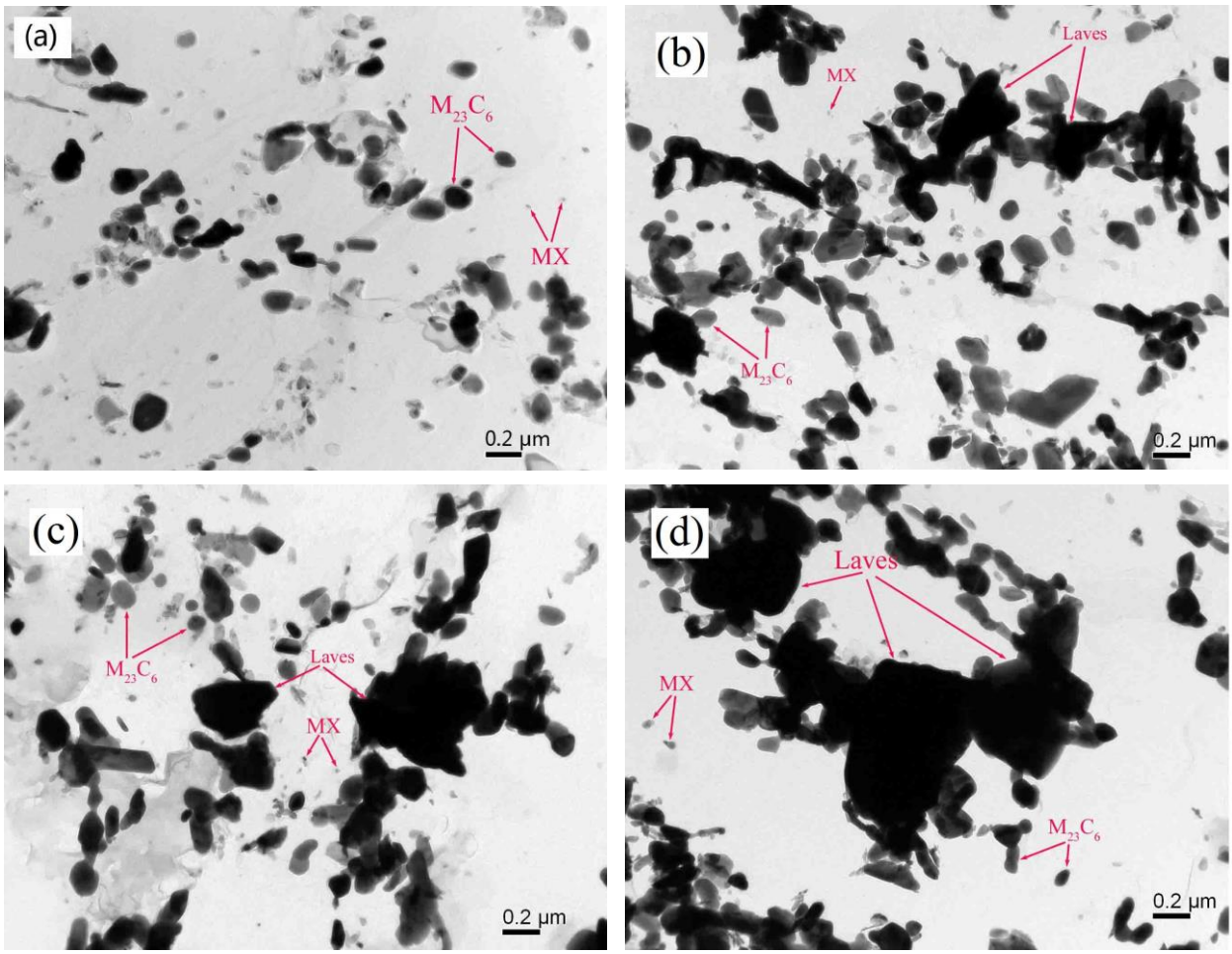

Fig.6 TEM micrographs of the replica of P92 steel. as received (a) and aged at 923 K for（b）500 h,（c）2000

h, (d) 5000 h

Fig.7 shows the identification of coarse precipitates by diffraction analysis with extraction replica from specimen aged at 923 K for 2000 h, revealing that the coarse precipitates are Laves-phase with primitive hexagonal crystal structure.

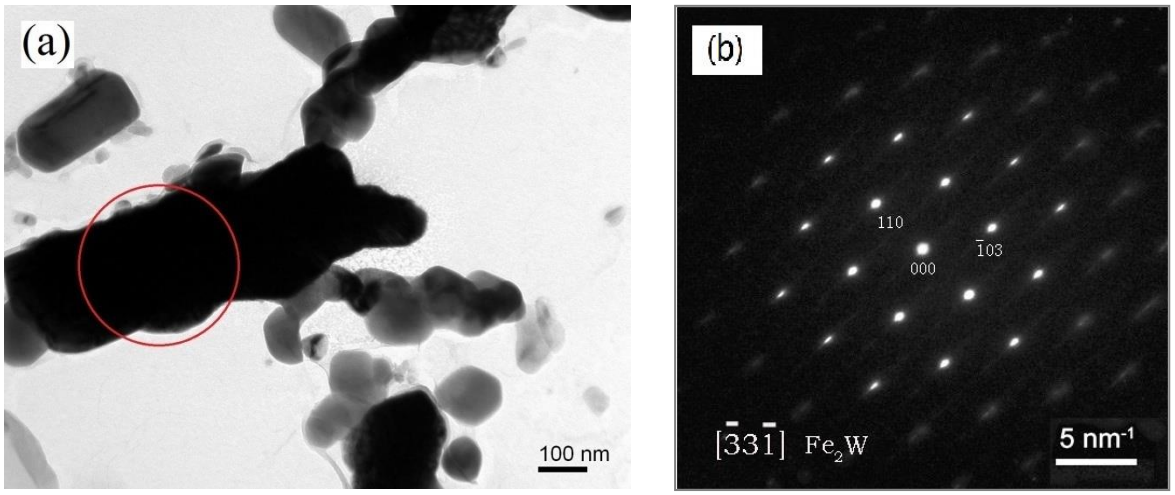

Fig.7 Identification of coarse precipitates by diffraction analysis with extraction replica from P92 steel aged at 923 K for 2000 h, (a) bright field image,（b）selected area diffraction pattern

Table 2 lists the average chemical composition of single Laves-phase precipitates by EDS under different aging conditions, together with metastable and equilibrium calculations by Thermo-Calc, indicating that, 1) Fe, Cr, Mo and W elements are present in Laves-phase, and ratio of（Fe、Cr）and (Mo、W）in at.% is around 2:1. 2) Laves-phase is a W-rich phase with higher W concentration than Mo. 3) The composition of Laves-phase remains unchanged during aging. A reasonable good agreement is found for the W concentration in Laves-phase between measured data by EDS and calculations by Thermo-Calc, but the difference of the other constituent elements seems to be relative large. Moreover, the formation of Z-phase has no effect at all on the composition of the Laves-phase, this may be due to the Z- phase containing no concentrations of Mo or W.

Table 2. Results from EDS analyse of Laves-phase (in normalised at.%)

Aging conditions	Cr	Fe	Mo	W
923 K, 500 h	14.50±1.72	47.97±1.45	8.54±0.79	28.95±1.04
923 K, 2000 h	17.07±3.42	47.25±1.75	8.15±0.90	27.53±1.48
923 K, 5000 h	13.46±2.15	49.36±1.59	8.12±0.56	29.06±1.28
Metastable equilibrium calculation (without the precipitated Z-phase)	9.60	56.88	3.98	29.18
Equilibrium calculation	9.60	56.88	3.98	29.18

Table 3 lists the mean chemical composition of single $M_{23}C_6$ by EDS under different aging conditions, showing that, 1) The metallic elements in $M_{23}C_6$ carbide mainly contain Fe and Cr, but some amount of W and Mo. 2) The change in the compositions of $M_{23}C_6$ is also little during aging. 3) The difference of Fe and Cr concentrations in $M_{23}C_6$ precipitates between measured data and calculations by Thermo-Calc is small, but measured values exhibit lower Mo content and slightly higher W content than calculations. No change in the compositions of $M_{23}C_6$ during aging indicates that the precipitation of Laves-phase does not affect the constituents of $M_{23}C_6$ carbide. In addition to the slower coarsening rate of $M_{23}C_6$ carbide mentioned above, this result further reveals that $M_{23}C_6$ carbide is a stable precipitate at 923K aging in P92 steel.

Table 3. EDS analyse of $M_{23}C_6$carbides (in normalised at.%)

Aging conditions	Cr	Fe	Mo	W	Mn	V
923 K, 500 h	67.61±1.12	22.72±0.90	2.0±0.24	5.29±0.33	1.35±0.28	1.03±0.62
923 K, 2000 h	68.09±1.80	22.41±1.37	1.91±0.16	5.40±0.36	1.41±0.24	0.78±0.27
923 K, 5000 h	69.86±1.25	19.71±0.76	1.97±0.22	5.64±0.46	1.35±0.26	1.47±0.96
Equilibrium calculations	69.92	18.04	7.10	3.34	0.35	1.24

3.4. Potentiostatic electrolysis Results

The contents of Cr, Mo, W, V and Nb in precipitates during aging, which are the constituents of $M_{23}C_6$, MX or Laves, are shown in Fig.8. It is found that a markedly increase in the Mo and W concentrations occurred in the

extracted residues as a result of precipitation of Laves-phase during aging for the first 1500 h. It should be noted that the increasing Cr content in the extracted residues can also be observed in this stage. The increase in Cr content during early stage aging is not probably ascribed to Cr-rich $M_{23}C_6$ carbides, because they have precipitated during tempering and their composition keep constant during aging. This can be explained by the precipitation of Laves-phase, because this phase also contains Cr apart from Mo and W, as shown in Table 2. As the aging time over 1500 h, the Mo and W concentrations in the extracted residues saturate due to the end of Laves-phase precipitation, in agreement with investigations based on SEM observations. In contrast, the contents of V and Nb, as the constituents of MX carbonitrides, are unchanged, indicating that this secondary type phases have precipitated during normalizing or tempering.

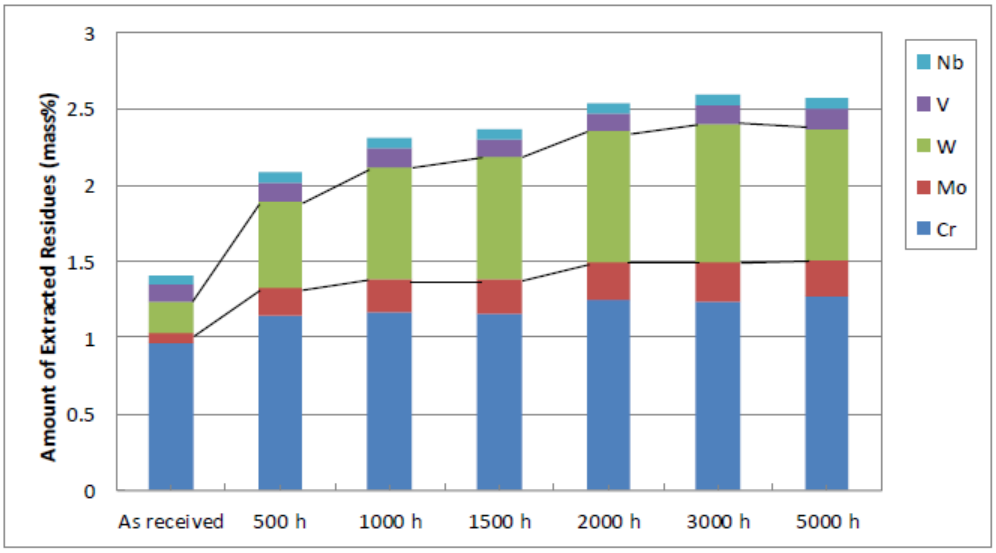

Fig.8 The amount and composition of extracted residues as a function of aging time for P92 steel at 923 K

Redistribution of Mo and W elements takes place due to the precipitation of Laves phase, resulting in the increase of Mo and W in precipitates and decrease of these two elements supersaturated in the matrix. The partition coefficient of alloying elements in the matrix is defined as follows:

$$\eta_i = \frac{C_0^{\,i} - C_0^{\,R} \times C_R^{\,i}}{C_0^{\,i}} \qquad (2)$$

where $C_0^{\,i}$ is wt.% of alloying element *i* in steel, $C_0^{\,R}$ is wt.% of extracted residues in steel, $C_R^{\,i}$ is wt.% of alloying

element *i* in extracted residues. Variations of partition coefficients of Mo and W in the matrix with aging time are shown in Fig.9. It is observed that partition coefficients of Mo and W drop rapidly with increasing time during the early aging stage. When aging time exceeds 1500 h, partition coefficients of the two elements in matrix retain a constant value of about 50%. Variations of partition coefficients of Mo and W in the matrix with aging time correspond well to the change of area fraction of Laves-phase (Fig.3a). It should be noted from Fig.9 that not all the Mo and W atoms of the steel are dissolved in the matrix before aging, with about 14 wt.% of Mo and W of the steel in precipitates. This is ascribed to $M_{23}C_6$ carbides formed during tempering before aging containing Mo and W atoms (as shown in Table 3). On the basis of the results of potentiostatic electrolysis, the significant depletion of Mo and W in the matrix is closely correlated with the precipitation of Laves-phase.

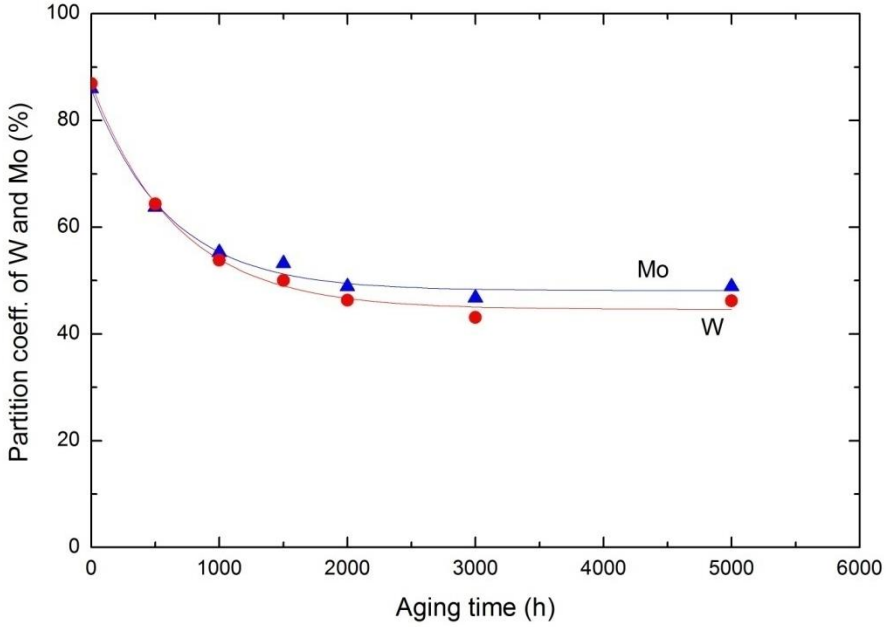

Fig.9 Varations of the partition coefficients of Mo and W supersaturated in matrix with aging time at 923 K for P92 steel

3.5. Hardness Measurement

Fig.10 shows the change of hardness as a function of aging time. The hardness of the as-received specimen is around 230 HB and gradually reduces to 213 HB of the specimen aged for 8000 h at 923 K. In the early stages of aging (below 2000 h) , although the fine Laves-phase may contribute to the precipitating hardening, the loss of

hardness seems to be more pronounced than after the aging time above 2000 h, and is in good agreement with the large drop of concentrations of Mo and W in the matrix, both of which decrease quickly because of the precipitation of Laves-phase (as shown Fig.9). After aging times beyond 2000 h, the concentrations of Mo and W atom keep a constant value in the matrix due to the completion of Laves-phase precipitation, and the drop of hardness becomes slow accordingly. This indicates that the depletion of dissolved atoms in the matrix caused by the precipitation of Laves-phase may be one of the main factors responsible for the drop in hardness in the early aging stage. The other microstructure changes including recovery of excess dislocations and coarsening of precipitates, mainly cause the continuing loss of hardness for the longer time aging. Lee et al [10] proposed to detect and investigate coarsening of Laves phase by means of hardness measurement of the steel exposed at elevated temperature and no stress. We agree with his proposal and confirm that the loss of hardness can be more clearly and easily detected in the precipitation of Laves-phase stages.

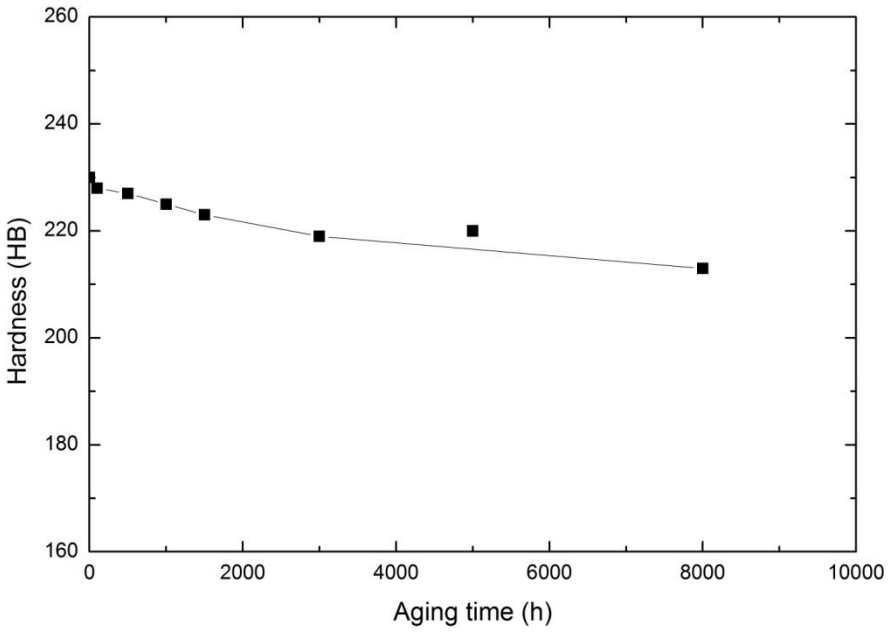

Fig.10 Change of hardness of P92 steel as a function of aging time at 923 K

4. Discussion

4.1. Kinetics of Laves-phase Precipitation and Coarsening

On the basis of the results reported above, Laves-phase precipitation in P92 steel occurs mainly during the first

1500 h of aging at 923 K. The time-dependent volume fraction *f* of a secondary phase can be described using the Johnson-Mehl-Avrami equation:

$$f(t) = 1 - e^{-(\frac{t}{t_0})^n} \qquad (3)$$

where t_0 is a time constant and *n* is a time exponent. The value of the time exponent *n* depends on the nucleation mechanism. In the case of secondary phase precipitates nucleating at boundaries, the time exponent is *n*=3/2 and 1/2 for the constant nucleation rate and nucleation rate rapidly decreasing to zero, respectively [18]. In Fig.11, the time exponent *n* has been evaluated according to experimental data of the test P92 steel based on the Johnson-Mehl-Avrami equation (Eq.(3)), thus deduces the nucleation mechanism for Laves-phase precipitation. The evaluation of the time exponent *n* and a time constant t_0 using a linear regression method on specimens up to an aging time of approximately 1500 h, shows a value of 0.67 for *n*, and a time constant t_0 to be approximately 5.5×10^9[s]. The time exponent *n* close to 1/2 suggests that the boundaries are the preferential nucleation sites of Laves-phase in P92 steel, which is in reasonable with results from observations by SEM images that Laves-phase precipitates on martensite laths boundaries and grain boundaries (Fig.2).

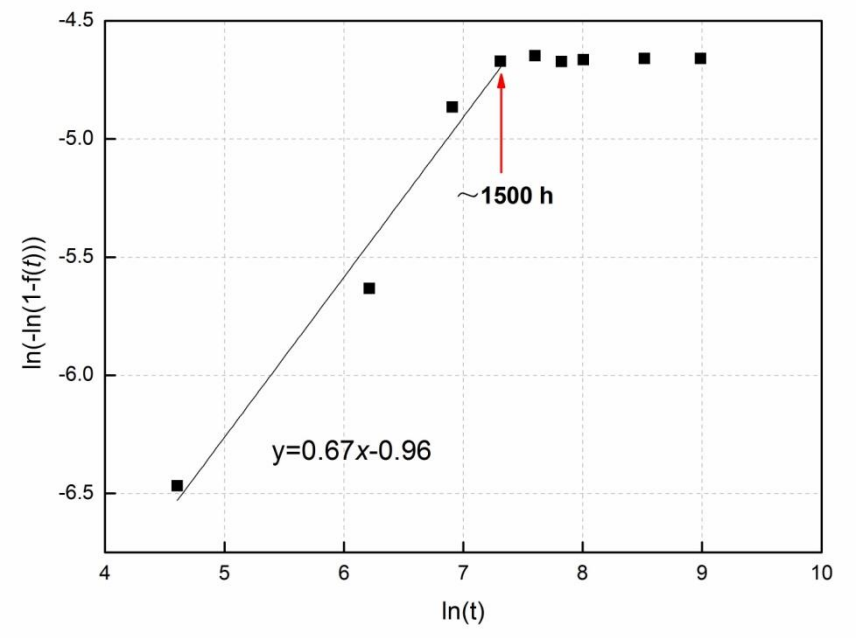

Fig.11 Evaluation of time exponent *n* based on the quantification results of the area fraction of Laves-phase precipitates in P92 steel at 923 K

The Laves-phase coarsening mechanism is discussed as follows. 1) Once the precipitation of Laves-phase is finished, the area fraction of Laves-phase keeps a constant value and a redistribution of particles takes place, which marks the beginning of coarsening. The coarsening is described by the following Ostwald ripening equation:

$$r^m - r_0^m = K_p t \qquad (4)$$

where r_0 and r is the average radius of particles at the beginning of coarsening and at a given time t, and K_p is a constant. The exponent m is 3 for coarsening controlled by volume diffusion. In a multi-phases system of β precipitate in the matrix, the coarsening rate constant K_p can be calculated theoretically by the following formula [19]:

$$K_p = \frac{8}{9} \frac{\gamma V_m^{\beta}}{\sum_{i=1}^{c} \frac{(x_i^{\beta} - x_i^{\alpha/\beta})^2}{x_i^{\alpha/\beta} D_i / RT}} \qquad (5)$$

In equation (5) γ is the interfacial energy and V_m^{β} is the molar volume of the precipitate phase. D_i is the diffusion coefficient of element i in the matrix, X_i^{β} is the molar fraction of element i in the precipitate and $X_i^{\alpha/\beta}$ is the molar fraction of element i at the precipitate /matrix interface (often used as X_i^{α}, the molar fraction of element i in the matrix). R is the gas constant and T is the temperature. The value of γ is 1 Jm^{-2} due to incoherent coarse Laves-phase particle/matrix interfaces. V_m^{β} =4.57×10^{-8} m^3 is for Laves phase, D_W=2.22×10^{-17} m^2/s and D_{Mo}=9.6×10^{-17} m^2/s are for α-Fe at 923 K. The values of X_i^{β} and X_i^{α} are evaluated using Thermo-Calc and they are 29.18% and 0.27%. The calculated value of K_p is 3.80×10^{-30} m^3/s using Eq.(5) in the case of m=3 (coarsening controlled by volume diffusion).

However, a theoretically calculated value of K_p is two orders of magnitude smaller than predicted by the experimental curve (Fig.12). Furthermore, Abe et al [20] have revealed that the volume diffusion controlled process is mainly involved in the coarsening of $M_{23}C_6$ carbides during creep based on the comparison of the

experimental results and calculations. Hald[21] reported that the theoretically calculated value of K_p for $M_{23}C_6$ is 4.78×10^{-30} m^3/s, which is slightly higher than that of K_p for Laves-phase in the case of m=3 at 923K in P92 steel, while Laves-phase exhibits a much rapider coarsening rate than $M_{23}C_6$ from our SEM observations. Therefore, it can be concluded that the Ostwald ripening of Laves-phase precipitates in P92 steel is not controlled apparently only by volume diffusion. Much higher diffusion coefficients of W and Mo element at grain boundaries than inside grain during Ostwald ripening, therefore, other diffusion mechanisms such as grain boundary diffusion, may accelerate its ripening. Lee et al [10] also suggested that grain boundaries is a diffusion path in the nucleation and coarsening of Laves-phase in P92 steel.

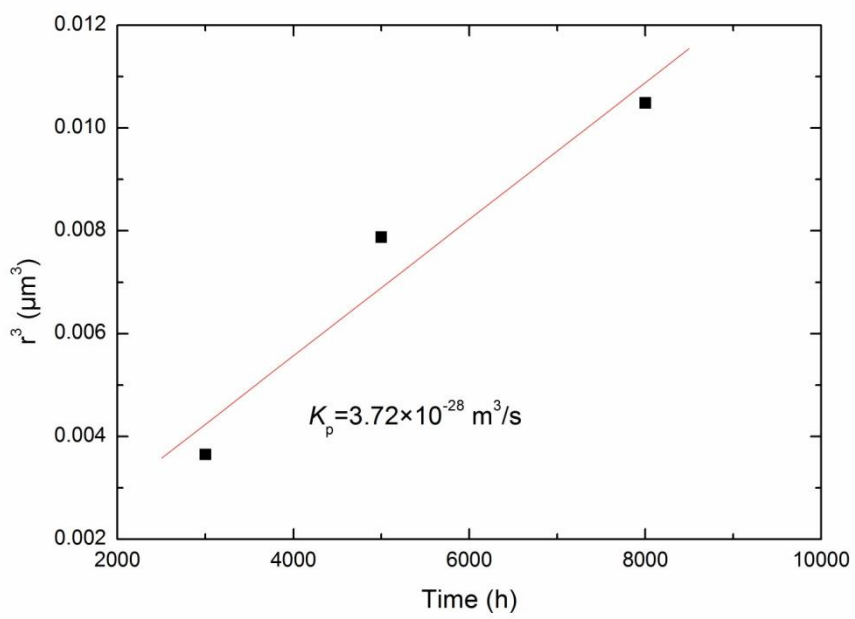

Fig.12 Coarsening rate constant of Laves-phase estimated from the experimental results in P92 steel at 923 K

4.2. Effect of Laves-phase Precipitation on Substructure and Creep Strength of Steel P92

In the early stage of aging, Laves-phase with relatively higher number density and smaller mean interparticle spacing, may improve creep strength by dispersion hardening. Precipitation hardening enhanced by retarding the recovery migration of dislocations and subgrain boundaries, is the most important method to increase the long-term creep strength of tempered martensitic 9%Cr steel. The Orowan stress due to precipitates is given by the following equation[22]:

$$\sigma_{Orowan} = 3.32Gb\frac{\sqrt{f_p}}{d_p} \qquad (6)$$

where G is the shear modulus (64 GPa at 923 K), b is the length of Burgers vector (0.25 nm), f_p is the precipitate volume fraction and d_p is the mean precipitate diameter. The Orowan stress of Laves-phase particles and $M_{23}C_6$ carbides by Eq.(6) is given in Table 4. It shows that the maximum Orowan stress produced by the Laves-phase precipitates takes place at the time for the completion of its precipitation, and below or beyond that time will fall due to the lower volume fraction or coarsening. It should be noted that the Orowan stress of Laves-phase precipitates is much lower than that of $M_{23}C_6$ carbides , only about its one fourth to one fifth.

Table 4. Orowan stress of precipitates estimated from the Eq.(5)

Particle	Volume fraction fp (%)	Diameter dp (nm)	Orowan stress σ_{or}（MPa）
Laves (923 K, 500 h)	0.36	241	13
Laves (923 K, 1500 h)	0.93	284	18
Laves (923 K, 8000 h)	0.94	438	12
$M_{23}C_6$ (Unaged) *	2.0	95	79
$M_{23}C_6$ (923 K, 3000 h) *	2.0	118	64
$M_{23}C_6$ (923 K, 10000 h)*	2.0	144	52

* In ref. [23]

The precipitation of Laves-phase during aging causes the reduction of Mo and W atoms supersaturated solute in the matrix. Solid solution strengthening is often discussed to explain the effect of Mo and W on creep strength of 9-12% Cr steel, but experimental evidence to demonstrate and quantify the mechanism is sparse. On the basis of the quantitative estimation as shown in Fig.8 and Fig.9, the drop of Mo and W dissolved in the matrix in the early stage of aging is very fast, and the loss of hardness is significant correspondingly although the precipitated Laves-phase brings about a certain amount of dispersion hardening. On the completion of Laves-phase precipitation, the amount of Mo and W in the matrix does not reduce any more, and the hardness drops slowly

correspondingly. The continuing drop in hardness may result from the recovery of excess dislocations and coarsening of the precipitates, including the $M_{23}C_6$ carbides and Laves-phase. This indirectly suggests that solid solution hardening enhanced by Mo and W atom is one of the main strengthening mechanism in P92 steel. Thus, it can be concluded that the effect of depletion of dissolved atoms in the matrix due to the precipitation of Laves-phase on creep strength should not be neglected.

In the present study, the much lower coarsening rate of $M_{23}C_6$ carbides than that of Laves-phase was observed during aging. Hald et al [21] have reported that the value of K_p for $M_{23}C_6$ carbides in P92 steel is one order lower than that in P91 steel. The addition of W in 9% Cr steel can suppress the coarsening of $M_{23}C_6$ carbides, although the mechanism by which this occurs is not fully understood [24]. $M_{23}C_6$ carbides mainly on lath boundaries retard the migration of subgrain boundaries, resulting in the significant precipitation hardening. Therefore, the stability of $M_{23}C_6$ carbides is crucial for avoiding the creep strength loss of P92 steel. In the present research, the maintaining of lath structure and relative slow drop of hardness during aging at 923 K in P92 steel are closely correlated with the thermally stable $M_{23}C_6$ carbides, and the contribution of precipitation hardening by the newly formed Laves-phase is small.

The above discussion is focused on the microstructural change and its influence on the capability of resisting creep deformation. However, it is necessary to point out that the final rupture of P92 material [10] and weld [11] is often associated with the cavitation that is one of the problems for which authors are advocating and working [9, 25]. The detailed information about creep cavity can be obtained by new techniques and examples of such work have been published [26].

Thus, future work is planned to investigate the thermal coarsening under stress and how it contributes to cavity nucleation and cavity growth under multi-axial states of stress.

5. Conclusions

The results of the precipitation and coarsening of Laves-phase in P92 steel during aging at 923 K can be summarized as follows.

1. SEM-BSE is a suitable method for measurement of Laves-phase precipitates, and can achieve significant statistical data when characterizing large particles comparing with the EFTEM, so that evaluate the kinetics of precipitation and coarsening of Laves-phase.
2. Laves-phase nucleates and grows rapidly within the first approximately 1,500 h of aging, and is found to be located at grain boundaries and martensite laths boundaries. The Laves-phase kinetics supports this conclusion. The saturated value of its volume fraction is around 0.95%.
3. Obvious coarsening of Laves-phase starts at approximately 3,000 h of aging and its rate is much greater than that of $M_{23}C_6$ carbides. Both the volume diffusion and the grain boundary diffusion control the Ostwald ripening of Laves-phase.
4. The precipitation of Laves-phase produces a pronounced matrix depletion of W and Mo atoms, and partition coefficients of these two elements supersaturated in the matrix reduce from 86% before aging to 50% on the completion of its precipitation.
5. The precipitating of Laves-phase causes the loss of hardenss and creep strength due to the depletion of Mo and W from the solid solution, and its precipitation strengthening is much weaker than $M_{23}C_6$ carbides.

References

[1]Bugge J.,Kjaer Sven,Blum R., Energy 2006;31：1437-45.

[2]Sheng Q., Liu H G., Electric Power Constrcution (China). 2010: 31: 71

[3]Muramatasa K., in :Viswanathan R, Nutting J (Eds), Proceedings of the Advanced Heat Resistant Steels for Power Generation, The University Press, Cambridge, 1998, P. 543.

[4]Yoshizawa M., Igarashi M., Moriguchi K., Iseda A., Armaki H G, Maruyama K., Mater. Sci. Eng. A 2009 ;510-511 :162-168.

[5]Hosoi Y., Wade N., Kunimitsu S., Urita T., J Nucl. Mater. 1986 ;461 :141-3.

[6]Ennis P J, Lipiec A Z, Wachter O., Filemonowicz A C, Acta Mater. 1997 ;45 :4901-7.

[7]Abe F., Mater Sci Eng A 2001 ;319-321 :770-773.

[8]Sawada K., Takeda M., Maruyama K., Ishii R., Yamada M., Nagae Y., Komine R., Mater. Sci. Eng. A 1999 ;267 :19-25.

[9]Xu Q., Lu Z., WANG X., Damage Modelling: the current state and the latest progress onthe development of creep damage constitutive equations for high Cr steels, in HIDA-6 Conference: Life/DefectAssessment&Failures in High Temperature Plant, 2nd - 4th December 2013, Nagasaki, Japan

[10]Lee J S, Armaki H G, Maruyama K,, Muraki T,, Asahi H., Mater. Sci. Eng. A 2006 ;428 :270-5.

[11]Wang X., Pan Q G., Ren Y Y., Zeng H Q., Liu H., Mater. Sci. Eng. A 2012 ;552 :493-501.

[12]Hofer P., Cerjak H., Warbichler P., Mater. Sci. Technol. 2000 ;16 :1221-5.

[13]Hättestrand M., Andrėn H O., Micron 2001 ;32 :789-97.

[14]DeHoff RT, Rhines FN, Method of estimating size of discrete objects. In : DeHoff RT, Rhines FN, editors. Quantitative microscopy. New York. McGraw-Hill ; 1968. p. 75-102.

[15]Fujita N., Ohmura K., Yamamoto A., Mater. Sci. Eng. A 2003 ;351 :272-81.

[16]Dimmler G., Weinert P., Kozeschnik E., Cerjak H., Mater. Charact. 2003 ; 51 :341-52.

[17]Danielsen H K., Hald J., Calphad 2007 ;31 :505-514.

[18] Long Q Y., Secondary phase in steels (China). Metallurgical Industry Press，Beijing, 2006.

[19]Ågren J., Clavaguera-Mora M T, Golcheski J., Inden G., Kumar H., Sigli C.,Calphad 2000 ;24 :41-54.

[20] Abe F., Mater. Sci. Eng. A 2004 ;387-389 :565-9.

[21] Hald J., Korcakova L., ISIJ International 2003 ;43 :420-7.

[22] Hald J.,J.Pres Ves Technol, 2008; 85: 30-37.

[23] Gustafson Å., Hättestrand M., Mater. Sci. Eng. A 2002 ;333 :279-86.

[24] Abe F., Sci. Technol. Adv. Mater. 2008 ;9 :1-15.

[25]Yang X., Xu Q., Lu Z Y., Donnelly, S., and Glove I, The relative signifiance of infernal damage mechanisms on the overall creep damage and ultimate failure of P91 steel, in HIDA-6 Conference: Life/DefectAssessment&Failures in High Temperature Plant, 2nd - 4th December 2013, Nagasaki, Japan

[26]Gupta C, Toda H, Schlacher C, Adachi Y, Mayr P, Sommitsch C, Uesugi K, Suzuki Y, Takeuchi A, Kobayashi M, Mater. Sci. Eng. A 2013, 564:525-538.

Acknowledgements

The authors would like to express their gratitude for projects supported by the National Natural Science Foundation of China (51074113 and 51374153) and Sichuan Province Fundamental Research Project （2013JY0123）.